**Med, Volume *2***

## Supplemental information

# Mucosal-associated invariant T cell responses differ by sex in COVID-19

**Chen Yu, Sejiro Littleton, Nicholas S. Giroux, Rose Mathew, Shengli Ding, Joan Kalnitsky, Yuchen Yang, Elizabeth Petzold, Hong A. Chung, Grecia O. Rivera, Tomer Rotstein, Rui Xi, Emily R. Ko, Ephraim L. Tsalik, Gregory D. Sempowski, Thomas N. Denny, Thomas W. Burke, Micah T. McClain, Christopher W. Woods, Xiling Shen, and Daniel R. Saban**

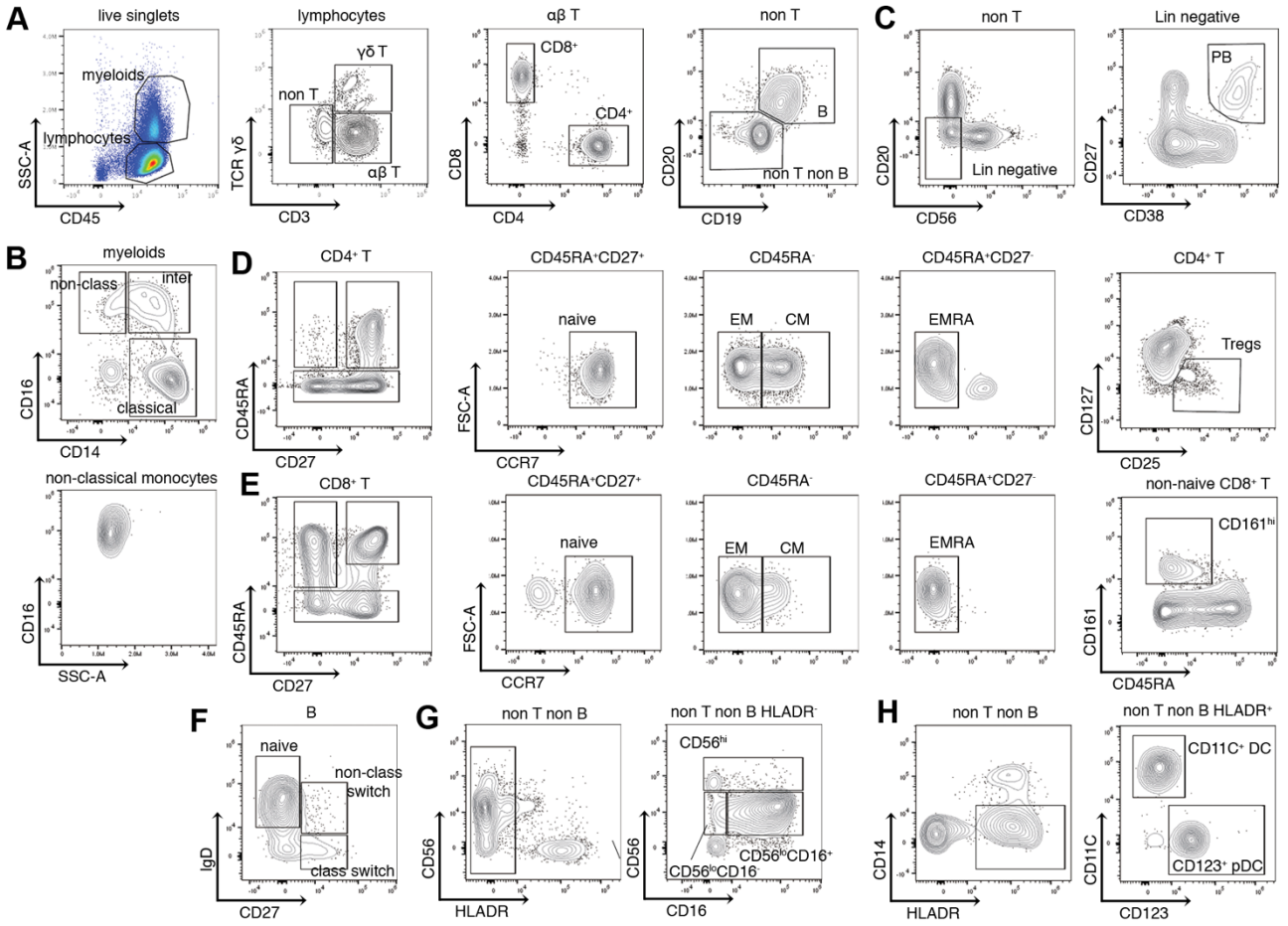
A
live singlets
myeloids
lymphocytes
SSC-A
CD45
lymphocytes
γδ T
non T
αβ T
TCR γδ
CD3
αβ T
CD8⁺
CD4⁺
CD8
CD4
non T
B
non T non B
CD20
CD19
C
non T
Lin negative
CD20
CD56
Lin negative
PB
CD27
CD38
B
myeloids
non-class
inter
classical
CD16
CD14
non-classical monocytes
CD16
SSC-A
D
CD4⁺ T
CD45RA
CD27
CD45RA⁺CD27⁺
naive
FSC-A
CCR7
CD45RA⁻
EM
CM
CD45RA⁺CD27⁻
EMRA
CD4⁺ T
Tregs
CD127
CD25
E
CD8⁺ T
CD45RA
CD27
CD45RA⁺CD27⁺
naive
FSC-A
CCR7
CD45RA⁻
EM
CM
CD45RA⁺CD27⁻
EMRA
non-naive CD8⁺ T
CD161ʰⁱ
CD161
CD45RA
F
B
naive
non-class switch
class switch
IgD
CD27
G
non T non B
CD56
HLADR
non T non B HLADR⁻
CD56ʰⁱ
CD56ˡᵒCD16⁺
CD56ˡᵒCD16⁻
CD56
CD16
H
non T non B
CD14
HLADR
non T non B HLADR⁺
CD11C⁺ DC
CD123⁺ pDC
CD11C
CD123
I
CD4⁺ T: naive
CD4⁺ T: CM
CD4⁺ T: EM
p = 0.0433
CD4⁺ T: EMRA
CD4⁺ T: Tregs
CD8⁺ T: naive
CD8⁺ T: CM
CD8⁺ T: EM
p = 0.0112
% CD45⁺ PBMCs
CD8⁺ T: EMRA
CD8⁺ T: CD161ʰⁱ
p = 0.0006
gd T
NK: CD56ʰⁱ
NK: CD56ˡᵒCD16⁻
p = 0.0247
NK: CD56ˡᵒCD16⁺
p = 0.0006
B: naive
p = 0.0015
B: class switch
% CD45⁺ PBMCs
B: non-class switch
p = 0.003
PB
p = 0.0002
CD11c⁺ DC
p < 0.0001
CD123⁺ pDC
p = 0.0004
classical MO
p = 0.0480
intermediate MO
p = 0.0367
nonclassical MO
p = 0.0037
% CD45⁺ PBMCs
healthy
exposed
infected
hospitalized

**Figure S1. Manual Gating Strategy and Immune Profiling of PBMC Subsets in COVID-19, Related to Figure 1.** (A-H) Gating strategy of major lymphocyte (A) and myeloid cell (B) subsets in PBMC samples, including CD4 (D) and CD8 (E) αβ T cells, γδ T cells (A), monocytes (B), B cells (F), plasmablasts (PB, C), NK cells (G) and dendritic cells (DC, H). (I) Frequencies of major PBMC subsets identified in A-H among healthy, exposed, infected and hospitalized groups. Significance was determined by Kruskal-Wallis test (p-values as indicated).

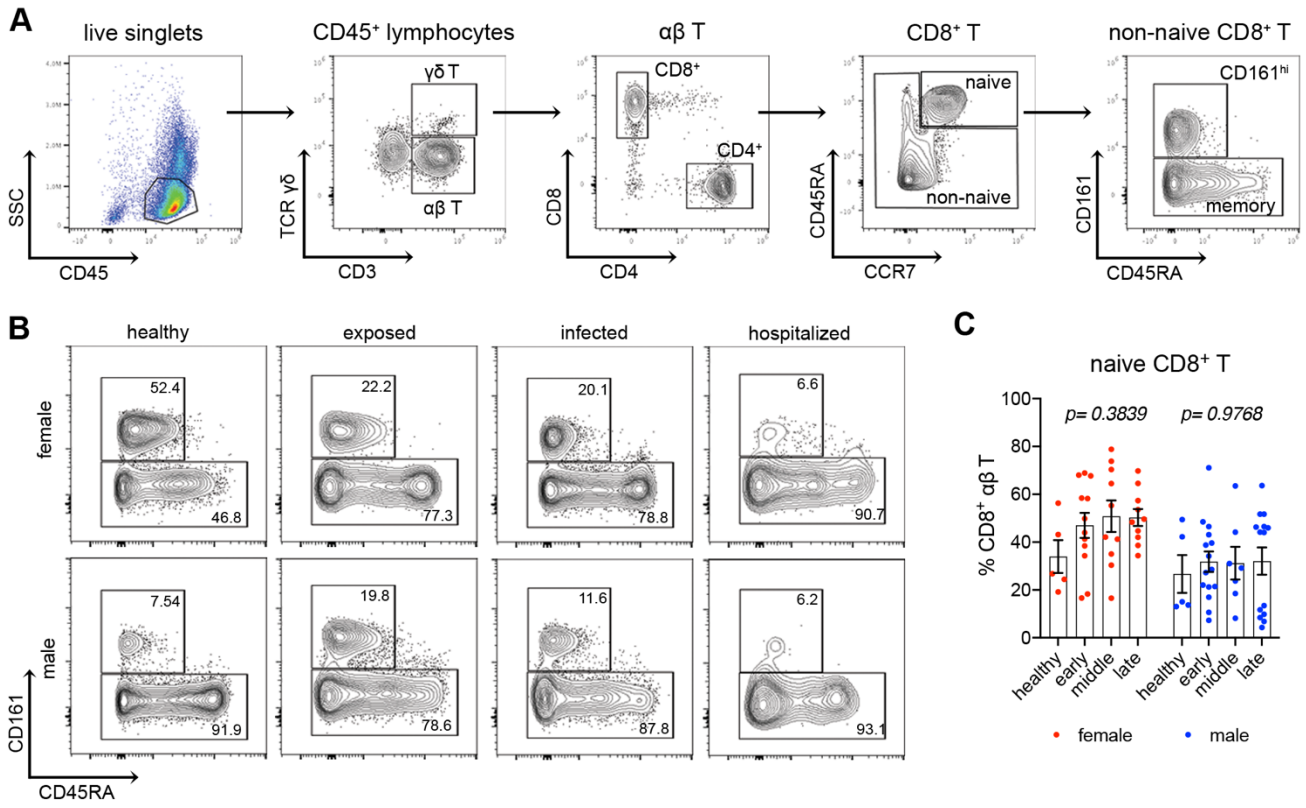


**Figure S2. Sex-Specific Changes of CD8⁺ CD161$^{hi}$ and Memory T Cells in COVID-19 PBMCs analyzed by Flow Cytometry, Related to Figure 2.** (A) Gating strategy of CD8⁺ CD161$^{hi}$ and memory T cells (αβ). (B) Representative flow plots of CD8⁺ CD161$^{hi}$ and memory T cells from female and male individuals with severity rank. (C) Frequencies of naïve CD8 T cells among different severity groups as indicated. Significance was calculated by Kruskal-Wallis.

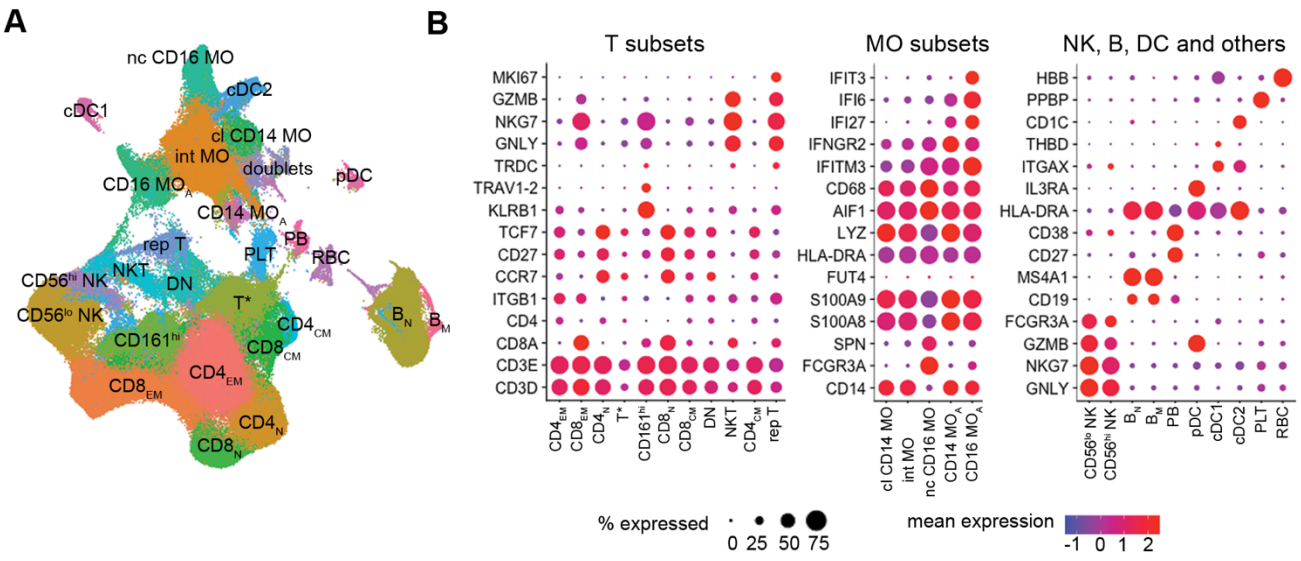


**Figure S3. Characterization of Immune Subsets in COVID-19 PBMCs by scRNA-seq, Related to Figure 3.** (A) High resolution clustering of PBMCs as shown in Figure 3A. (B) Expression of marker genes used to annotate the identifies of individual clusters. N, naïve; EM, effect memory; CM, central memory; DN, double negative; rep, replicating. cl, classical; int, intermediate; nc, non-classical; CD14 $MO_A$, activated CD14 monocytes; CD16 $MO_A$, activated CD16 monocytes; NK, natural killer; PB, plasmablasts; PLT, platelets; DC, dendritic cells.

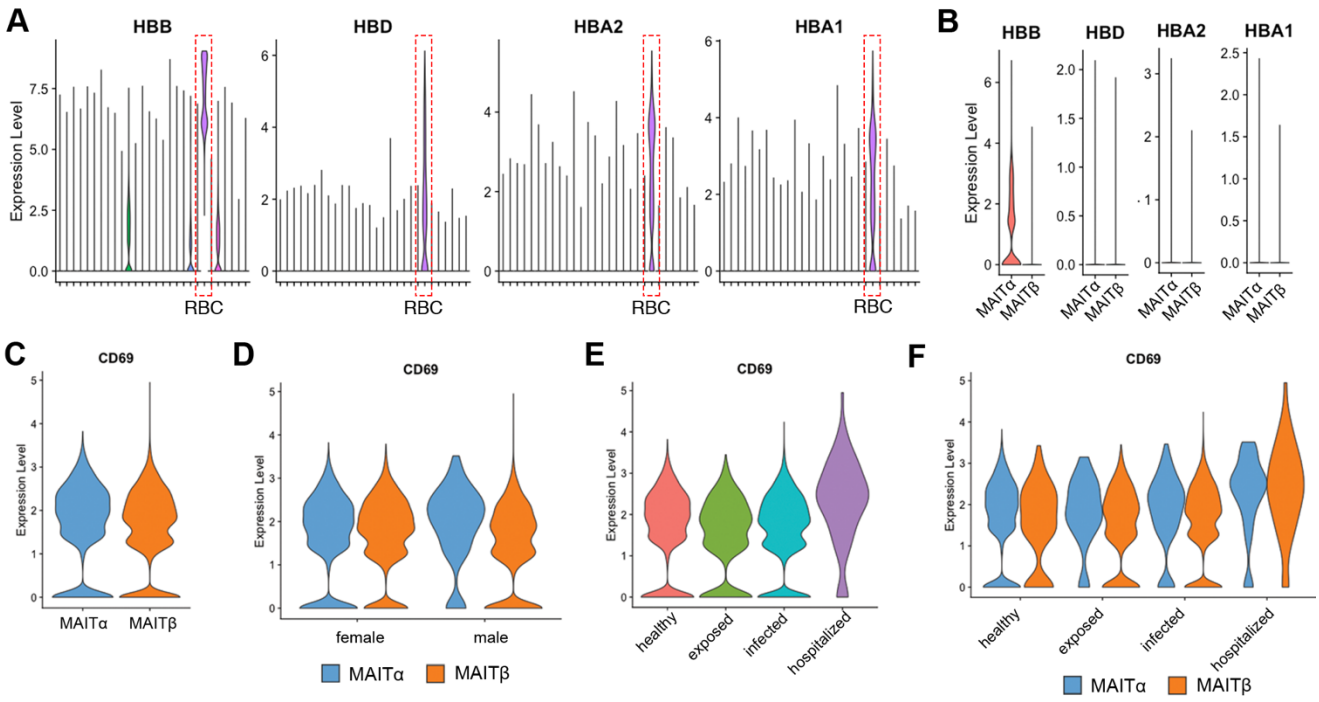


**Figure S4. Expression of HBB and CD69 by Circulating MAIT Clusters in COVID-19, Related to Figure 5**. (**A,B**) Expression of hemoglobin related genes (*HBB, HBD, HBA2, HBA1*) are shown by PBMC clusbters (A) and MAIT clusters (B). Red dash boxes indicates RBC cells. (C to F) Data are grouped by MAIT clusters (C), sex (D), severity rank (E) as well as clusters and severity (F).

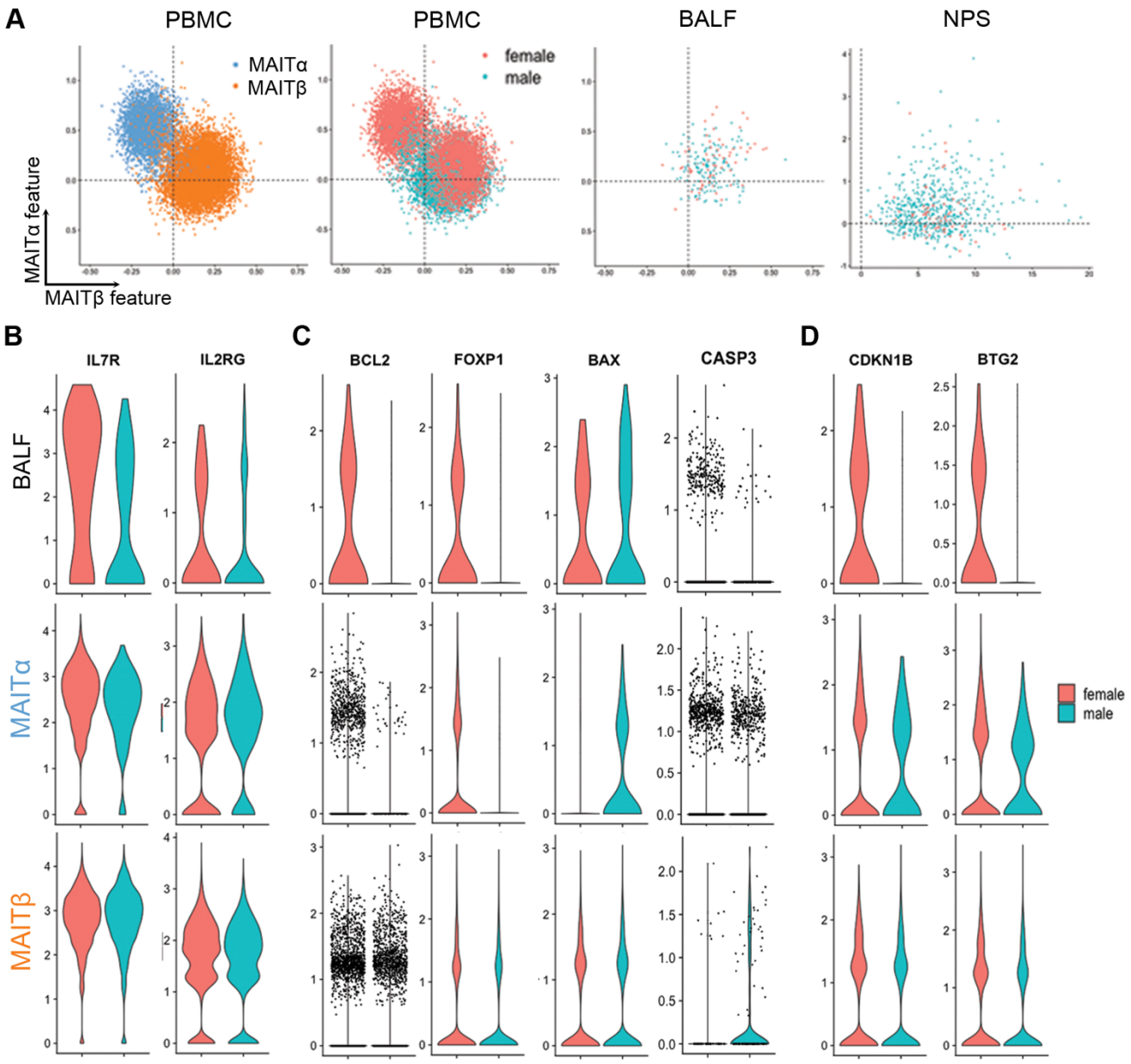


**Figure S5. Comparisons of MAITα and MAITβ Features in MAIT Cells from Peripheral Blood and Airway Tissue Samples, Related to Figure 6.** (A) Estimation of MAITα and MAITβ features of individual cells from PBMC and BALF dataset based on the expression of MAITα gene (y-axis) and MAITβ gene sets (x-axis). Differentially expressed genes between MAITα and MAITβ were used as two modular features, respectively. (B to D) Expression of IL7

receptor and its co-receptor genes (B), apoptosis-related genes (C), proliferation-related genes by MAIT cells from PBMC and BALF dataset (D).

**Table S1. Clinical Metadata of Participants and Samples in this study, Related to Figure 1 and Table 1.** Clinical data of participants in the 1st sheet 1; sample metadata in the 2nd sheet.

**Table S2. List of DEGs of PBMC Clusters, Related to Figure 3.** The DEGs of each PBMC cluster are listed with details of p-values (p_val), average log2 fold changes (avg_logFC), percentages of cells with the detected feature (pct.1 and pct.2), clusters and gene names.

**Table S3. List of DEGs of MAIT Subsets, Related to Figure 4.** The DEGs of MAITα and β are listed with details of p-values (p_val), average log2 fold changes (avg_logFC), percentages of cells with the detected feature (pct.1 and pct.2), clusters and gene names.

**Table S4. List of Enriched Reactome Pathways of MAIT Subsets, Related to Figure 4.** Details of the parameters provided by Reactome Pathway enrichment analysis. MAITα in the 1st sheet 1; MAITβ, the 2nd sheet.